as light yellow plates. Yield: 31.3 g (88%). Anal. Calcd for $TiC_{32}H_{36}O_4$: C, 72.16; H, 6.83. Found: 72.05; H, 7.27. ^1H NMR. (C_6D_6, 30 °C): δ 2.20 (s, CH_3); 6.7-7.2 (m, aromatics).

3. Zr(OAr-*i*-Pr$_2$)$_4$ (3). To a colorless solution of $Zr(CH_2SiMe_3)_4$ (1.5 g; 3.4 mmol) in hexane (15 mL) was slowly added 2,6-diisopropylphenol (2.7 g; 15.1 mmol). The solution became warm and was allowed to cool down before being reduced in volume by one-half, whereupon white crystals of product began to form. The crystals were removed and washed with a small amount of cold hexane. Yield: 1.0 g (37%). Anal. Calcd for $ZrC_{48}H_{68}O_4$: C, 72.03; H, 8.58. Found: C, 70.99; H, 8.41. ^1H NMR. (C_6D_6, 30 °C): δ 1.15 (d, CHMe_2); 3.60 (septet, CHMe$_2$); 6.7-7.2 (m, aromatics).

4. [(thf)$_2$Na·Ti(OAr-*i*-Pr$_2$)$_4$] (4). A yellow-gold solution of (1) (3.0 g, 3.96 mmol) in thf rapidly became deep green on addition of sodium amalgam (1.1 equiv of Na). After the mixture was stirred at room temperature for 2 h, the resulting green solution was decanted from the mercury and the solvent removed to give the crude product. Yield: 3.0 g (96%). Recrystallization can be readily achieved from hot toluene, yielding light blue crystals. Anal. Calcd for $TiC_{56}H_{84}O_6Na$: C, 72.77; H, 9.18. Found: C, 69.83; H, 8.90.

5. Ti(OAr-*i*-Pr$_2$)$_3$(py)$_2$ (5). To a dark green solution of (4) (0.50 g; 0.54 mmol) in toluene (10 mL) was added pyridine (0.1 mL). The resulting deep purple mixture was stripped to dryness and extracted with 160 mL of a 6:1 mixture of hexane/toluene to give 0.32 g of crude product (81%). Recrystallization from toluene gave 0.10 g of deep purple needles. Anal. Calcd for $TiC_{46}H_{61}O_3N_2$: C, 74.86; H, 8.35; N, 3.80. Found: C, 75.59; H, 7.90; N, 3.65.

X-ray Crystallography

General operating procedures have been reported previously.[17]

Ti(OAr-*i*-Pr$_2$)$_4$ (1). A systematic search of a limited hemisphere revealed a set of diffraction maxima with monoclinic symmetry. An initial assignment of $P2_1/a$ was discovered to be incorrect after data collection had been in progress for some time, as body centering was present. The correct space group was then identified as $I2/a$, and no attempt was made to convert it to the standard setting ($C2/c$).

The structure was solved by direct methods and Fourier techniques and refined by full-matrix least squares. All hydrogen atoms were located and refined isotropically (anisotropic refinement for Ti, C, and O). A final difference Fourier was featureless, the largest peak being 0.32 e/Å^3. No attempt was made to correct the data for absorption.

[Ti(OAr-*i*-Pr$_2$)$_4$·Na(thf)$_2$] (4). Crystals of this complex diffracted only weakly. Hence, the results obtained, although not as accurate as one expects, represent the best we have been able to achieve. A small well-formed crystal was selected and transferred to the diffractometer, where it was cooled to −159 °C and characterized in the usual manner. A systematic search of a limited hemisphere of reciprocal space yielded a set of reflections which exhibited orthorhombic symmetry. The systematic extinctions of $h00$ for h odd, $0k0$ for k odd, and $00l$, for l odd identified the space group as $P2_12_12_1$.

The structure was solved by a combination of direct methods and heavy-atom techniques. The Ti and Na atoms were located by direct methods, and the remaining atoms were located by successive difference Fourier maps. The structure was refined by full-matrix least squares. Ti, Na, and O atoms were assigned anisotropic thermal parameters. Hydrogen atoms were not located but were introduced in calculated fixed positions. The refinements were carried out by using only 1810 reflections having $F > 2.33\sigma(F)$. The number of unique reflections was 3911.

The enantiomer shown in this report was selected from refinements of both enantiomers; however, the difference in R was quite small.

Acknowledgment. We thank the National Science Foundation (Grant CHE-8219206 to I.P.R.) for support of this research.

Registry No. 1, 99398-78-4; 2, 49796-02-3; 3, 99398-79-5; 4, 99398-81-9; 5, 99398-82-0.

Supplementary Material Available: Listings of hydrogen atom parameters, anisotropic thermal parameters, complete bond distances and angles, coordination data for Ti and Na, and observed and calculated structure factors (37 pages). Ordering information is given on any current masthead page.

(17) Huffman, J. C.; Lewis, L. N.; Caulton, K. G. *Inorg. Chem.* **1980**, *19*, 2755.

(18) In this paper the periodic group notation is in accord with recent actions by IUPAC and ACS nomenclature committees. A and B notation is eliminated because of wide confusion. Groups IA and IIA become groups 1 and 2. The d-transition elements comprise groups 3 through 12, and the p-block elements comprise groups 13 through 18. (Note that the former Roman number designation is preserved in the last digit of the new numbering: e.g., III 3 and 13.)

Contribution from the Department of Chemistry, The University of North Carolina, Chapel Hill, North Carolina 27514

Structural Variations Induced by Changes in Oxidation State and Their Role in Electron Transfer. Crystal and Molecular Structures of *cis*-[Ru(bpy)$_2$Cl$_2$]·3.5H$_2$O and *cis*-[Ru(bpy)$_2$Cl$_2$]Cl·2H$_2$O

Drake S. Eggleston, Kenneth A. Goldsby, Derek J. Hodgson,* and Thomas J. Meyer*

Received October 26, 1984

The results of an X-ray crystallographic study are reported on the hydrates *cis*-[Ru^{II}(bpy)$_2$Cl$_2$]·3.5H$_2$O and *cis*-[Ru^{III}(bpy)$_2$Cl$_2$]Cl·2H$_2$O (bpy is 2,2′-bipyridine, $C_{10}H_8N_2$). The Ru(II) complex crystallizes in the monoclinic space group $C2/c$ with four molecules in a cell of dimensions a = 18.248 (14) Å, b = 13.146 (5) Å, c = 10.792 (4) Å, and β = 119.49 (5)° and was refined to a final value of the weighted R factor of 0.031 based on 1912 independent observations. The Ru(III) complex crystallizes in the triclinic space group $P\bar{1}$ with two molecules in a cell of dimensions a = 7.042 (3) Å, b = 13.000 (5) Å, c = 12.321 (3) Å, α = 89.93 (2)°, β = 100.62 (2)°, and γ = 92.23 (3)° and was refined to a weighted R factor of 0.033 based on 2104 independent observations. In terms of intramolecular structure, there is a significant shortening (0.10 Å) of the Ru–Cl bond upon oxidation and a slighter *increase* (0.04 Å) in the Ru–N distances trans to the Ru–Cl bonds. An analysis of the contribution of intramolecular vibrations to the vibrational barrier to electron transfer for the [Ru(bpy)$_2$Cl$_2$]$^{+/0}$ couple is presented based on the structures and available vibrational information. The lattice structure of the hydrate [Ru(bpy)$_2$Cl$_2$]·3.5H$_2$O is notable both for the appearance of bpy-based stacking interactions between neighboring molecules and for the existence of an infinite chain of H-bonded water molecules. The latter exists as an aqueous channel within the crystal, individual water molecules of which are H-bonded to bound Cl$^-$.

Introduction

Complexes of Ru(II) and Ru(III) have played an important role in the study of optical and thermal electron transfer because of coordinative stability in both oxidation states.[1,2] From current theory, the activation energy to electron transfer is a function of the energy required to modify the solvent structure around the reactants, the electrostatic energy of interaction between the reactants, and the inner-sphere reorganization energy. The in-

(1) (a) Creutz, C. *Prog. Inorg. Chem.* **1983**, *30*, 1. (b) Meyer, T. J. *Acc. Chem. Res.* **1978**, *11*, 94.

(2) Richardson, D. E.; Walker, D. D.; Sutton, J. E.; Hodgson, K. O.; Taube, H. *Inorg. Chem.* **1979**, *18*, 2216.

0020-1669/85/1324-4573$01.50/0

ner-sphere term depends on the changes in the equilibrium coordinates of the normal modes and the associated normal mode frequencies.

For metal complexes, normal modes largely M–L stretching in character play an important role, and the use of crystallographically derived metal–ligand bond distance changes has aided in the estimation of inner-sphere reorganizational barriers for such couples as $[Ru(NH_3)_6]^{3+/2+}$,[3] $[Co(NH_3)_6]^{3+/2+}$,[4] $[Fe(phen)_3]^{3+/2+}$,[5] $[Fe(H_2O)_6]^{3+/2+}$,[6] $[Ru(H_2O)_6]^{3+/2+}$,[7] and Ru(II/III) pentaammine and tetraammine couples with π-acid ligands.[2,8,10,11]

Most of the structural applications to theory to date have been based on octahedral or approximately octahedral cases such as $[Co(NH_3)_6]^{3+/2+}$ [11a] or $[Fe(H_2O)_6]^{3+/2+}$.[10,11b] These cases are relatively easy to treat theoretically since near-octahedral symmetry is maintained in both oxidation states. This means that, of the largely metal–ligand-based normal modes, only the totally symmetrical metal–ligand "breathing" mode can make a significant contribution to vibrational trapping of the transferring electron. That this is so follows from the fact that only for νa_{1g}(M–L) is the change in the equilibrium normal coordinate between oxidation states, ΔQ_{eq}, nonzero. Although contributions to vibrational trapping arise from any normal mode for which there is either a change in ΔQ_{eq} *or* a change in frequency between oxidation states, even slight changes in ΔQ_{eq} are normally a far more important factor.[11,12]

For lower symmetry cases the problem can be far more difficult in terms of defining both the normal modes of the system and the appropriate combination of normal modes needed to interconvert the structures of the two oxidation states. Although difficult to treat, most redox systems involve couples of lower symmetry and/or complex changes in structure exist between oxidation states induced by the difference in electron content. With a few exceptions,[13,14] detailed analyses on more complex systems are unavailable.

In this paper we present the crystal and molecular structures of the complexes *cis*-$[Ru(bpy)_2Cl_2]$ and *cis*-$[Ru(bpy)_2Cl_2]Cl$ (bpy is 2,2′-bipyridine). Complexes of this type have been especially important in mixed-valence complexes and the study of optical charge transfer.[1] We were interested in exploring the structural changes induced between oxidation states with an eye toward helping to define the role of intramolecular vibrational trapping in these systems.

Experimental Section

Measurements. The infrared spectrum of *cis*-$[(bpy)_2Ru^{III}Cl_2]Cl$ was obtained by using a Beckman IR 4250 recording spectrophotometer. CsI plates were used, with the sample being ground in Nujol.

Table I. Crystallographic Parameters for *cis*-$[Ru(bpy)_2Cl_2]\cdot 3.5H_2O$ and *cis*-$[Ru(bpy)_2Cl_2]Cl\cdot 2H_2O$

	Ru(II)	Ru(III)
space group	$C2/c$	$P\bar{1}$
a, Å	18.248 (14)	7.042 (3)
b, Å	13.146 (5)	13.000 (5)
c, Å	10.792 (4)	12.321 (3)
α, deg		89.93 (2)
β, deg	119.49 (5)	100.62 (2)
γ, deg		92.23 (3)
V, Å^3	2254 (5)	1107 (1)
Z	4	2
D_c, g cm^{-3}	1.59	1.67
D_m, g cm^{-3}	1.58 (1)[a]	1.65 (1)[b]
μ, cm^{-1} (Mo Kα)	9.473	10.792
N_o ($I \geq 3\sigma(I)$)	1912	2104
N_v	180	291
R	0.033	0.043
R_w	0.031	0.033
GOF	1.64	1.29
max cor to F^2	1.029	1.122
min cor to F^2	1.001	1.004
2θ limits, deg	2–55	2–50
T, °C	19	19
octants collcd	$\pm h,+k,+l$	$+h,\pm k,\pm l$

[a] By flotation in $CHCl_3/CCl_4$. [b] By flotation in 1,3-dibromopropane/CCl_4.

Materials. $RuCl_3\cdot 3H_2O$ was purchased from Bishop-Matthey and used as received. All other chemicals and solvents were reagent grade and used without further purification.

Preparation of $[Ru(bpy)_2Cl_2]\cdot 3.5H_2O$. The complex $Ru(bpy)_2Cl_2$ was prepared by a literature procedure.[15] Deep purple crystals were grown by slow evaporation of a saturated aqueous ethanol solution at room temperature. Due to some uncertainity in the molecular formula that arose during the crystal structure determination, a sample of these crystals was sent for elemental analysis. The results (Galbraith Labs) were consistent with a molecular formula that includes at least three but fewer than four waters of crystallization. Anal. Calcd for $[Ru(bpy)_2Cl_2]\cdot 3.5H_2O$: C, 43.88; H, 4.24; N, 10.24. Found: C, 44.17; H, 4.53; N, 10.20.

Preparation of $[Ru(bpy)_2Cl_2]Cl\cdot 2H_2O$. $RuCl_3\cdot 3H_2O$ (1.57 g, 6.0 mmol) and 2,2′-bipyridine (1.873 g, 11.99 mmol) were combined in 30 mL of absolute ethanol and heated at reflux for 12 h while magnetic stirring was maintained. After this time, the reaction mixture was allowed to cool to room temperature, and a brown solid was isolated by suction filtration. The crude product was added to 700 mL of a very hot solution of LiCl (30 g) in H_2O and allowed to stir for 15 min. The solution was filtered hot, and the filtrate volume was reduced to one-third on a rotary evaporator, yielding brownish orange crystals. The crystalline product was isolated by suction filtration, washed with a small portion of cold H_2O, and transferred to a vacuum desiccator. Yield: 0.527 g (17% based on $RuCl_3\cdot 3H_2O$). Anal. Calcd for $[(bpy)_2RuCl_2]Cl\cdot 2H_2O$: C, 43.21; H, 3.27; N, 10.08. Found: C, 43.00; H, 3.31; N, 10.05. Tabular orange plates of the dihydrate were grown by slow room-temperature evaporation of a hot aqueous 2-propanol solution of the complex, which had been filtered to remove insoluble impurities and to which a small quantity of LiCl had been added. Crystals of this material displayed a marked tendency to grow in pairs or to exhibit twinning.

Collection and Reduction of X-ray Data. A prismatic crystal of the Ru(II) complex of approximate dimensions 0.70 × 0.40 × 0.40 mm and a thin plate of the Ru(III) complex of approximate dimensions 0.15 × 0.40 × 0.40 mm were used for data collection on an Enraf-Nonius CAD-4 diffractometer using Mo Kα radiation and a graphite monochromator. Cell parameters are given in Table I along with other pertinent crystallographic information.

For both crystals, the data were corrected for background, Lorentz–polarization effects, and absorption as described elsewhere.[16] The maximum and minimum absorption correction factors employed for both crystals are listed in Table I.

Solution and Refinement of the Structures. Both structures were solved by employing Patterson techniques and difference Fourier syntheses. The Patterson map for the Ru(II) data indicated, as expected, that the Ru atom sat on a C_2 axis at 0, y, $^1/_4$. After refinement of this initial position,

(3) (a) Stynes, H. C.; Ibers, J. A. *Inorg. Chem.* **1971**, *10*, 2304. (b) Meyer, T. J.; Taube, H. *Inorg. Chem.* **1968**, *7*, 2369.
(4) (a) Stranks, D. R. *Discuss. Faraday Soc.* **1960**, *29*, 116. (b) Hammershoi, A.; Geselowitz, D.; Taube, H. *Inorg. Chem.* **1984**, *23*, 979–982.
(5) (a) Zalkin, A.; Templeton, D. H.; Ueki, T. *Inorg. Chem.* **1973**, *12*, 1641. (b) Baher, J.; Englehardt, L. M.; Figgis, B. N.; White, A. H. *J. Chem. Soc., Dalton Trans.* **1975**, 530.
(6) (a) Hair, N. J.; Beattie, J. K. *Inorg. Chem.* **1977**, *16*, 245. (b) Beattie, J. K.; Best, S. P.; Skelton, B. W.; White, A. H. *J. Chem. Soc., Dalton Trans.* **1981**, 2105. (c) Brunschwig, B. S.; Creutz, C.; McCartney, D. H.; Sham, T.-K.; Sutin, N. *Faraday Discuss. Chem. Soc.* **1982**, *74*, 113.
(7) Bernhard, P.; Burgi, H.-B.; Hauser, J.; Lehmann, H.; Ludi, A. *Inorg. Chem.* **1982**, *21*, 3936.
(8) Gress, M. E.; Creutz, C.; Quicksall, C. O. *Inorg. Chem.* **1981**, *20*, 1522.
(9) Bottcher, W.; Brown, G. M.; Sutin, N. *Inorg. Chem.* **1979**, *18*, 1477.
(10) (a) Newton, M. D.; Sutin, N. *Annu. Rev. Phys. Chem.* **1984**, *35*, 437. (b) Sutin, N. *Prog. Inorg. Chem.* **1983**, *30*, 441.
(11) (a) Buhks, E.; Bixon, M.; Jortner, J.; Navon, G. *Inorg. Chem.* **1979**, *18*, 2014. (b) Brunschwig, B. S.; Logan, J.; Newton, M. D.; Sutin, N. *J. Am. Chem. Soc.* **1980**, *102*, 5798.
(12) Ballhausen, C. J. "Molecular Electronic Structures of Transition Metal Complexes"; McGraw-Hill: New York, 1979; Chapter 4.
(13) Fischer, S. F.; VanDuyne, R. P. *Chem. Phys.* **1977**, *26*, 9.
(14) (a) Caspar, J. V.; Westmoreland, T. D.; Allen, G. H.; Bradley, P. G.; Meyer, T. J.; Woodruff, W. H. *J. Am. Chem. Soc.* **1984**, *106*, 3492. (b) Poizat, O.; Sourisseau, C. *J. Phys. Chem.* **1984**, *88*, 3007. (c) Lipari, N. O.; Rice, M. J.; Duke, C. B.; Bozio, R.; Girlando, A.; Pecile, C. *Chem. Phys. Lett.* **1976**, *44*, 236; *Int. J. Quantum Chem., Quantum Chem. Symp.* **1977**, *11*, 583.
(15) Sullivan, B. P.; Salmon, D. J.; Meyer, T. J. *Inorg. Chem.* **1978**, *17*, 3334.
(16) Graves, B.; Hodgson, D. J. *Acta Crystallogr., Sect. B: Struct. Crystallogr. Cryst. Chem.* **1982**, *B38*, 135.

Table II. Fractional Atomic Coordinates for *cis*-$[Ru(bpy)_2Cl_2]\cdot 3.5H_2O$

atom	*x*	*y*	*z*
Ru	0.0000	0.20811 (3)	0.2500
Cl	0.07660 (4)	0.07666 (7)	0.42415 (7)
O(1)W	0.1069 (2)	0.0994 (2)	0.7433 (2)
O(2)W	0.0000	0.2688 (6)	0.7500
O(3)W	0.0000	0.4318 (13)	0.7500
N(1)	0.0983 (1)	0.2160 (2)	0.2086 (2)
N(1)′	0.0724 (1)	0.3149 (2)	0.3911 (2)
C(2)	0.1600 (2)	0.2827 (2)	0.2899 (3)
C(3)	0.2306 (2)	0.2936 (3)	0.2741 (3)
C(4)	0.2381 (2)	0.2386 (3)	0.1736 (3)
C(5)	0.1766 (2)	0.1711 (3)	0.0937 (3)
C(6)	0.1082 (2)	0.1612 (3)	0.1133 (3)
C(6)′	0.0569 (2)	0.3625 (3)	0.4858 (4)
C(5)′	0.1083 (2)	0.4351 (3)	0.5785 (4)
C(4)′	0.1808 (2)	0.4609 (3)	0.5764 (4)
C(3)′	0.1994 (2)	0.4119 (3)	0.4842 (4)
C(2)′	0.1452 (2)	0.3391 (2)	0.3920 (3)

with *x* and *z* fixed, difference Fourier maps gave positions for all expected heavy atoms based on the dihydrate formula reported previously in the literature. Following these initial cycles of refinement, a difference Fourier map indicated significant peaks, which lay on the twofold axis approximately 2.3 Å apart and clearly distant from ruthenium. These peaks were assigned as water oxygen atoms with multiplicities of 0.50 and 0.25, accounting for an additional $1^1/_2$ waters per ruthenium as indicated by the elemental analysis (vide supra). Hydrogen atom positions for H attached to the unique bipyridine ring were calculated from theoretical considerations, assuming a C–H bond length of 0.95 Å. These positions were confirmed by examination of a difference Fourier map after refinement of all heavy-atom positions with anisotropic librational parameters. Chemically reasonable positions for the two independent hydrogen atoms of one water molecule and the unique hydrogen atom of the full water molecule, which sits on the twofold axis, were also located in the Fourier map. A position for the hydrogen atom of the half-occupancy water molecule could not be located; however, this result is not unexpected considering the high thermal motion displayed by this randomly distributed oxygen. In the final cycles of least-squares refinement the positions of all hydrogen atoms, except those on the water molecules, were refined. Isotropic temperature factors for all hydrogen atoms were also refined.

For the Ru(III) structure, solution of the Patterson map and subsequent difference Fourier syntheses gave positions for all heavy atoms including two water oxygens. As for the Ru(II) structure, positions for the bipyridine ring hydrogen atoms were calculated from theoretical considerations and were confirmed through examination of a difference Fourier map. Positions for all four hydrogens attached to the two waters of crystallization were also observed. In subsequent least-squares cycles the calculated positions for hydrogen atoms attached to bipyridine rings, as well as those positions observed in the Fourier map for water hydrogen atoms, were held fixed. Isotropic temperature factors for all hydrogen atoms were refined.

Refinement, by full-matrix least-squares methods using scattering factors for non-hydrogen atoms taken from the ref 17a and hydrogen atom scattering factors from Stewart, Davidson, and Simpson[18] and including the real and imaginary parts of anomalous dispersion for all atoms,[17b] was carried out in each case in the centrosymmetric space group. The functions minimized were $\sum(|F_o| - |F_c|)/\sum|F_o|$ and $[\sum(|F_o| - |F_c|)^2/\sum(F_o)^2]^{1/2}$ where the weights, *w*, were initially assigned as unity but were eventually assigned as $w = 4F_o^2/\sigma^2(F_o^2)$ with $\sigma(F_o^2)$ given by $\sigma(F_o^2) = [\sigma^2(I) + p^2I^2]^{1/2}$ and *p* assigned the value 0.01 for our instrument. Final values of *R* and R_w are given in Table I.

In the final cycle of least squares no parameter shifted more than 0.03 and 0.49 times its estimated standard deviation for the Ru(II) and Ru(III) structures, respectively. A final difference Fourier map showed no peak higher than 0.33 e Å^{-3} for the Ru(II) structure and 0.25 e Å^{-3} for the Ru(III) structure. In each case the highest peaks were very close to either Ru or Cl atoms and presumably represent an inefficiency in our fitting of the correct thermal motion for these atoms or some slight inadequacy in the absorption correction. The final positional parameters along with their standard deviations (as estimated from the inverse least-squares matrix) are given in Tables II and III, for the Ru(II) and Ru(III) structures, respectively. Tables of anisotropic thermal parameters and observed and calculated structure amplitudes are available as supplementary material.

Table III. Fractional Atomic Coordinates for *cis*-$[Ru(bpy)_2Cl_2]Cl\cdot 2H_2O$

atom	*x*	*y*	*z*
Ru	0.10438 (9)	0.37151 (5)	0.21471 (5)
Cl(1)	0.3503 (2)	0.4318 (1)	0.3562 (1)
Cl(2)	0.2488 (3)	0.4479 (1)	0.0770 (1)
Cl(3)	0.1113 (3)	0.0372 (2)	0.7702 (2)
O(1)W	0.4022 (8)	0.1009 (4)	0.6086 (5)
O(2)W	0.2732 (8)	0.0155 (4)	0.3990 (4)
N(1)A	0.2381 (7)	0.2410 (4)	0.1813 (4)
N(1)A′	−0.1028 (7)	0.3011 (4)	0.0944 (4)
N(1)B′	−0.0405 (7)	0.3136 (4)	0.3328 (4)
N(1)B′	−0.0406 (7)	0.4972 (4)	0.2484 (4)
C(2)A	0.1484 (9)	0.1865 (5)	0.0914 (5)
C(3)A	0.2317 (9)	0.1022 (5)	0.0543 (5)
C(4)A	0.4054 (10)	0.0743 (5)	0.1104 (6)
C(5)A	0.4952 (10)	0.1278 (5)	0.2032 (6)
C(6)A	0.4098 (9)	0.2127 (5)	0.2360 (5)
C(2)A′	−0.0429 (9)	0.2204 (5)	0.0414 (5)
C(3)A′	−0.1600 (10)	0.1774 (5)	−0.0513 (5)
C(4)A′	−0.3383 (10)	0.2140 (5)	−0.0885 (6)
C(5)A′	−0.4019 (9)	0.2920 (5)	−0.0327 (6)
C(6)A′	−0.2819 (9)	0.3348 (5)	0.0585 (5)
C(2)B	−0.1352 (9)	0.4858 (5)	0.3351 (5)
C(3)B	−0.2253 (9)	0.5671 (5)	0.3719 (5)
C(4)B	−0.2179 (10)	0.6615 (5)	0.3212 (6)
C(5)B	−0.1201 (10)	0.6729 (5)	0.2349 (6)
C(6)B	−0.0332 (9)	0.5896 (5)	0.2020 (5)
C(2)B′	−0.1346 (9)	0.3827 (5)	0.3822 (5)
C(3)B′	−0.2193 (9)	0.3543 (5)	0.4708 (5)
C(4)B′	−0.2146 (10)	0.2545 (5)	0.5069 (5)
C(5)B′	−0.1179 (10)	0.1844 (5)	0.4553 (6)
C(6)B′	−0.0334 (10)	0.2156 (5)	0.3688 (5)

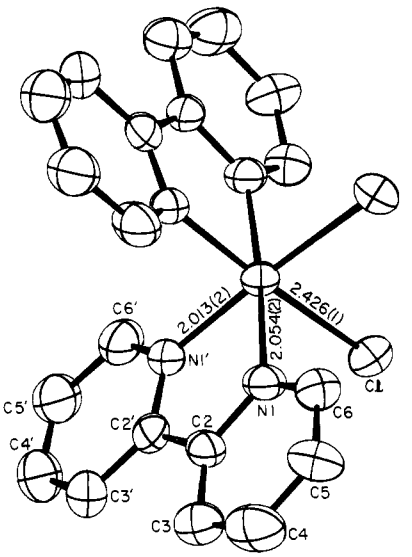

Figure 1. View of the $[Ru(bpy)_2Cl_2]$ molecule in the $[Ru(bpy)_2Cl_2]\cdot 3.5H_2O$ crystals. Thermal ellipsoids are drawn at the 50% probability level; the hydrogen atoms on bipyridine rings are omitted.

Results and Discussion

Views of the molecular units of *cis*-$[Ru(bpy)_2Cl_2]$ and *cis*-$[Ru(bpy)_2Cl_2]^+$ are provided in Figure 1 and Figure 2, respectively. As may be appreciated from a comparison of these figures, both molecular units exhibit almost idealized geometries with only slight distortions from rectilinear angles. The molecules shown in the figures have the Δ configuration at ruthenium, but in these centrosymmetric space groups there are an equal number of molecules displaying the Λ configuration within the cell. Unique bond distances within the coordination sphere of each molecule are included in the figures, and bond angles at ruthenium are given

(17) Ibers, J. A.; Hamilton, W. C. "International Tables for X-ray Crystallography"; Kynoch Press: Birmingham, England, 1974; Vol. IV: (a) Table 2.2A, pp 72–98, and Table 2.2C, p 102; (b) Table 2.3.1, pp 149–150.

(18) Stewart, R. F.; Davidson, E. R.; Simpson, W. T. *J. Phys. Chem.* **1965**, *42*, 3176.

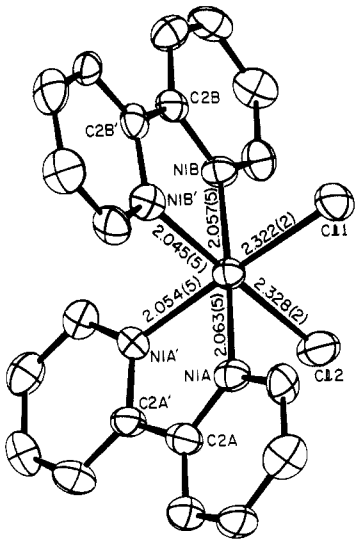

Figure 2. View of the $[Ru(bpy)_2Cl_2]^+$ cation in the $[Ru(bpy)_2Cl_2]Cl \cdot 2H_2O$ crystals. Thermal ellipsoids are drawn at the 50% probability level; hydrogens on bipyridine rings are omitted.

Table IV. Bond Angles (deg) at Ruthenium in *cis*-$[Ru(bpy)_2Cl_2] \cdot 3.5H_2O$ and *cis*-$[Ru(bpy)_2Cl_2]Cl \cdot H_2O$[a]

	$[Ru^{II}(bpy)_2Cl_2]$		
Cl–Ru–N(1)	88.44 (6)	Cl–Ru–N(1)	95.70 (6)
Cl–Ru–N(1)′	89.83 (6)	Cl–Ru–N(1)′	174.73 (7)
N(1)–Ru–N(1)′	79.10 (9)	N(1)–Ru–N(1)′*	96.81 (9)
N(1)–Ru–N(1)*	174.20 (13)	N(1)′–Ru–N(1)′*	91.63 (12)
Cl–Ru–Cl*	89.16 (13)		
	$[Ru^{III}(bpy)_2Cl_2]^+$		
Cl(1)–Ru–Cl(2)	93.7 (1)	N(1)A–Ru–N(1)A′	78.5 (2)
Cl(1)–Ru–N(1)A	95.6 (2)	N(1)A–Ru–N(1)B′	99.2 (2)
Cl(1)–Ru–N(1)A′	173.3 (2)	N(1)A–Ru–N(1)B	177.3 (2)
Cl(1)–Ru–N(1)B	86.1 (2)	N(1)A′–Ru–N(1)B′	89.8 (2)
Cl(1)–Ru–N(1)B′	88.1 (2)	N(1)A′–Ru–N(1)B	99.7 (2)
Cl(2)–Ru–N(1)A	85.4 (1)	N(1)B–Ru–N(1)B′	78.8 (2)
Cl(2)–Ru–N(1)B	96.7 (2)		
Cl(2)–Ru–N(1)B′	175.0 (2)		

[a] Starred atoms are related by C_2 symmetry to the position in Table II.

in Table IV. Other bond distances and angles are available as supplementary material.

$[Ru(bpy)_2Cl_2] \cdot 3.5H_2O$. The ruthenium atom in this molecule lies on a crystallographic twofold axis, thus a rigorous twofold symmetry is imposed on the Ru(II) molecular unit. Consequently, there is a unique chloride and a unique bipyridine ring per molecular unit.

The Ru(II)–Cl bond length of 2.426 (1) Å is longer than might otherwise have been expected in a compound of this type. Thus, this bond length is 0.035–0.055 Å longer than Ru(II)–Cl bonds observed in a number of structures in which chloride is trans to σ-donor ligands such as Cl^-, benzoate, or sulfate and is nearly 0.07 Å longer than the Ru(II)–Cl[19-23] bond trans to the strong π-acceptor ligand NO^+.[21] The shortening in the latter has been rationalized[21] by noting that Cl^- is a much stronger σ-donor than is NO^+. Since bipyridine is a relatively weak π-acid[24] whose σ-donor capacity is not expected to be significantly greater than that of chloride ion at Ru(II), little lengthening of the Ru–Cl bond trans to bipyridine is expected. This prediction is confirmed by the structure[25] of $[Ru(bpy)_2(CO)Cl]^+$, in which the Ru–Cl bond length is 2.396 (7) Å. The present value of 2.426 (1) Å is much longer than this value and is comparable to values observed[26] when Cl^- is trans to ligands that exert a strong trans influence owing to metal–ligand $d\pi$–$p\pi$ mixing. Part of the lengthening may arise from the relatively electron-rich nature of the Ru site compared to the nature of the nitrosyl or carbonyl complexes, but as is noted below, an additional contribution may arise from intermolecular hydrogen bonding interactions.

A notable feature of the $[Ru(bpy)_2Cl_2]$ structure is the difference of 0.041 Å between the two types of Ru–N bonds. The Ru–N(1) bond length for the nitrogen atom trans to another bipyridine nitrogen atom is 2.054 (2) Å, which is nearly the same as the value of 2.056 (2) Å observed in the structure of $[Ru(bpy)_3]^{2+}$.[27] The Ru–N(1)′ bond length for the nitrogen atom trans to chloride is 2.013 (2) Å in $[Ru(bpy)_2Cl_2]$, which is significantly shorter than Ru–N(1) and is the shortest Ru–N(bpy) bond length observed to date. The distinct shortening compared to the Ru–N bond trans to a bipyridine nitrogen atom may reflect the importance of Ru → N(bipyridine) π back-bonding. For a bipyridine nitrogen atom trans to a second bipyridine nitrogen atom a competition exists for election density involving the same filled $d\pi$ orbitals. For a bipyridine nitrogen atom trans to Cl, Cl^- is not a competitor for back-bonding and may, in fact, be at least a weak π-donor as well as a σ-donor.

The manifestations of $d\pi$–π^* metal to ligand back-bonding on chemical and physical properties in π-acid complexes of Ru(II) have been well documented.[28-30] In addition, there is a wealth of crystallographic data that supports the occurrence of back-bonding in Ru(II) complexes containing π-acceptors.[31-33]

Similar observations have been made, although not always commented on in related structures; as examples: (1) in the structure of $[Ru(bpy)_2(CO)(Cl)]^+$[25] the difference between Ru–N distances trans to bipyridine nitrogen and the Ru–N distance trans to Cl is 0.034 Å; (2) in the structure of *cis*-dichloro(1,4,8,11-tetrathiacyclotetradecane)ruthenium(II) the difference between the Ru–S distance trans to sulfur and the Ru–S distance trans to Cl is 0.071 Å.[34] These examples clearly illustrate the fallacy of applying arguments based on *average* bond distances to systems of lower symmetry in which there is a net electronic asymmetry, especially in cases where metal–ligand back-bonding is important.

The geometry of the $[Ru(bpy)_2Cl_2]$ molecule is as close to octahedral as possible considering the chelation requirements of the bipyridine ligand. The observed bpy "bite angle" of 79.1 (1)° is comparable to chelating angles observed normally for this ligand.[23,35] The cis-chloro angle of 89.16 (3)° is very nearly the ideal octahedral angle of 90° and is comparable to values observed in other cis-chloro Ru(II) structures.[19,22,23,25,34,36] As a consequence

(19) (a) McGuiggan, M. F.; Pignolet, L. H. *Cryst. Struct. Commun.* **1981**, *10*, 1227. (b) McGuiggan, M. F.; Pignolet, L. H. *Cryst. Struct. Commun.* **1978**, *7*, 583.
(20) Reed, J.; Soled, S. L.; Eisenberg, R. *Inorg. Chem.* **1974**, *13*, 3001.
(21) (a) Veal, J. T.; Hodgson, D. J. *Inorg. Chem.* **1972**, *11*, 1420. (b) Veal, J. T.; Hodgson, D. J. *Acta Crystallogr., Sect. B: Struct. Crystallogr. Cryst. Chem.* **1972**, *B28*, 3525.
(22) Haymore, B. L.; Ibers, J. A. *Inorg. chem.* 1975, *14*, 3060.
(23) Schultz, A. J.; Henry, R. L.; Reed, J.; Eisenberg, R. *Inorg. Chem.* **1974**, *13*, 732.
(24) Pipes, D.; Meyer, T. J. *Inorg. Chem.* **1984**, *23*, 2466.
(25) (a) Clear, J. M.; Kelly, J. M.; O'Connell, C. M.; Vos, J. G.; Cardin, C. J.; Costa, S. R.; Edwards, A. J. *J. Chem. Soc., Chem. Commun.* **1980**, 750. (b) McMillan, R. S.; Mercer, A.; James, B. R.; Trotter, J. *J. Chem. Soc., Dalton Trans.* **1975**, 1006.
(26) Vogt, L. H.; Katz, J. L.; Wiberley, E. W. *Inorg. Chem.* **1965**, *4*, 1157.
(27) Rillema, D. P.; Jones, D. S.; Levy, H. A. *J. Chem. Soc., Chem. Commun.* **1979**, 849.
(28) Ford, P.; Rudd, F. P.; Gaunder, R.; Taube, H. *J. Am. Chem. Soc.* **1968**, *90*, 1187.
(29) (a) Ford, P. C. *Coord. Chem. Rev.* **1970**, *5*, 75. (b) Zwickel, A. M.; Creutz, C. *Inorg. Chem.* **1971**, *10*, 2395.
(30) Taube, H. In "Survey of Progress in Chemistry"; Academic Press: New York, 1973; Vol. 6, p 1.
(31) Bottomley, F. *J. Chem. Soc., Dalton Trans.* **1972**, 2148; *Ibid.*, **1974**, 1600.
(32) Treitel, I. M.; Flood, M. T.; Marsh, R. E.; Gray, H. B. *J. Am. Chem. Soc.* **1969**, *91*, 6512.
(33) Cotton, F. A.; Edwards, W. T. *Acta Crystallogr., Sect. B: Struct. Crystallogr. Cryst. Chem.* **1968**, *B24*, 474.
(34) Lai, T.-F.; Poon, C.-K. *J. Chem. Soc., Dalton Trans.* **1982**, 1465.
(35) (a) Phelps, D. W.; Kahn, M.; Hodgson, D. J. *Inorg. Chem.* **1975**, *14*, 2486 and references therein. (b) Gilbert, J. A.; Eggleston, D. S.; Murphy, W. R.; Geselowitz, D. A.; Gersten, S. W.; Hodgson, D. J.; Meyer, T. J. *J. Am. Chem. Soc.* **1985**, *107*, 3855.
(36) Gould, R. O.; Jones, C. L.; Robertson, P. R.; Stephenson, T. A. *J. Chem. Soc., Dalton Trans.* **1977**, 129.

Table V. Probable Hydrogen-Bonding Interactions in *cis*-$[Ru(bpy)_2Cl_2]\cdot 3.5H_2O$ and *cis*-$[Ru(bpy)_2Cl_2]Cl\cdot 2H_2O$

bond	lengths, Å		angle, deg
	$[Ru(bpy)_2Cl_2]\cdot 3.5H_2O$		
Cl···H(1)O(1)W–O(1)W	Cl···O(1)W	3.222 (3)	164 (2)
	Cl···H(1)O(1)W	2.46	
Cl···H(2)O(1)W–O(1)W	Cl···O(1)W	3.246 (3)	157 (2)
	Cl···H(2)O(1)W	2.57	
O(1)W···HO(2)W–O(2)W	O(1)W···O(2)W	2.985 (7)	142 (2)
	O(1)W···HO(2)W	2.27	
O(2)···O(3)W		2.14 (2)	
	$[Ru(bpy)_2Cl_2]Cl\cdot 2H_2O$		
Cl(3)···H(1)O(1)W–O(1)W	Cl(3)···O(1)W	3.187 (7)	153 (2)
	Cl(3)···H(1)O(1)W	2.40	
Cl(3)···H(2)O(2)W–O(2)W	Cl(3)···O(2)W	3.140 (6)	175 (2)
	Cl(3)···H(2)O(2)W	1.93	
O(1)W···H(1)O(2)W–3(2)W	O(1)W···O(2)W	2.829 (9)	145 (2)
	O(1)W···H(1)H(1)O(2)W	2.08	

of the constraint of the bpy bite angle, the bipyridine ligands are bent back from the coordinated chlorides as can be seen in Figure 1 and as shown by the N(1)–Ru–N(1)′ angle of 174.2 (1)°, which is distorted from linearity by approximately 6°.

Bond lengths and angles within the bipyridine rings (available as supplementary material) are normal for the ligand and unworthy of further comment except to note the consistency in distances and angles between "chemically equivalent" atoms of the two pyridine rings. The bipyridine ring is virtually planar with no atom deviating from the 12-membered least-squares plane by more than 0.024 (4) Å. Each individual 6-membered pyridine ring is also virtually planar, maximum deviations being 0.011 (4) and 0.012 (2) Å for the unprimed and primed ring, respectively. The dihedral angle between pyridine planes is 1.3°.

The distinctive molecular packing arrangement within the $[Ru(bpy)_2Cl_2]\cdot 3.5H_2O$ lattice is probably facilitated by the planar bipyridine groups. Each individual molecular unit participates in two separate stacking interactions with neighboring molecules through one of the two pyridine rings of the bipyridine ligand. Thus, in one direction, the A rings of molecules related by an inversion center and the translation ($^1/_2$, $^1/_2$, 1) are stacked with an interplanar separation averaging 3.463 (3) Å. In a second, perpendicular direction, the A′ rings of molecules related by an inversion center and a unit cell translation along the *b* axis are stacked with an interplanar separation averaging 3.498 (3) Å. This two-dimensional, pairwise stacking arrangement presumably arises from favorable $\pi-\pi$ interactions between bipyridine rings and is probably facilitated by the neutral character of the Ru(II) molecule. A literature search indicates that such a packing arrangement has not been observed previously in structural studies of bipyridine or bipyridine–metal complexes. A similar, but distinct, packing arrangement involving overlapping phenanthroline rings occurs in crystals of $[Fe(phen)_3](ClO_4)_3\cdot H_2O$.[5b] The packing arrangement observed in the $[Ru(bpy)_2Cl_2]$ structure may provide a glimpse of the type of intermolecular interactions that can occur in solution and that could play a role in such processes as electron delocalization, kinetics of substitution, and exciplex formation. For example, Cayley and Margerum have documented large rate enhancements in complex formation reactions, which can be attributed directly to stacking interactions.[37] In principle, the observed packing interaction provides an electronic delocalization pathway throughout the lattice and the interaction itself could play a role in electron transfer as a preferred outer-sphere configuration or perhaps in exciplex formation involving excited states. In addition, similar ring–ring interactions have been observed structurally in dimeric polypyridyl complexes of Ru(III),[35] which may play a role in the activation of these complexes toward the catalyzed oxidation of H_2O and Cl^-.

There is an extensive hydrogen bonding network within the $[Ru(bpy)_2Cl_2]\cdot 3.5H_2O$ crystal, which is interesting because it may reveal details of the solution structure of this Ru complex in hydrogen-bonding solvents. Hydrogen bonding involving the coordinated chlorides is depicted in Figure 3. A table of metrical parameters for all hydrogen bonds is provided in Table V. Monomers of $[Ru(bpy)_2Cl_2]$ related by inversion centers are linked through hydrogen bonding between the coordinated chlorides and the full occupancy water, O(1)W, in an infinite chain along a direction parallel to the *c* axis. Each chloride participates in two hydrogen bonds to water, resulting in nearly symmetrical bridges between ruthenium monomers with Cl···O distances averaging 3.234 (3) Å and an associated Cl···O···Cl angle of 125.9 (1)°. The water oxygen O(1)W in turn acts as an acceptor from water O(2)W (the full-occupancy water on the twofold axis); thus O(1)W participates in three hydrogen bonds. The H-bonding scheme is completed by interactions between the two water molecules occupying positions on the twofold axis. Water oxygen O(3)W (the half-occupied position) apparently acts as a double donor to O(2)W below it such that O(2)W also participates in a tetrahedral hydrogen bonding interaction. The resulting O(2)W···O(3)W distance, 2.14 (2) Å, is a very close contact and undoubtedly is underestimated due to the considerable thermal motion of the two atoms and the probable random distribution

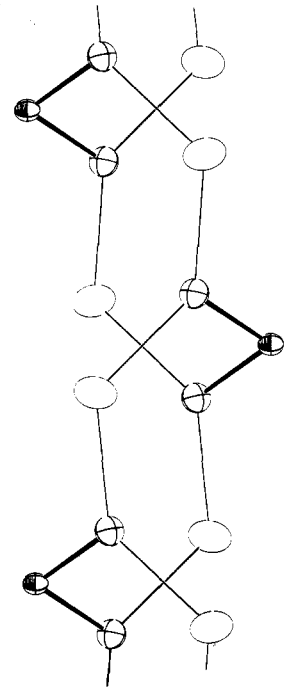

Figure 3. Hydrogen bonding involving chlorine and water in $[Ru(bpy)_2Cl_2]\cdot 3.5H_2O$. Ruthenium (shaded), chlorine (crosshatched), and water oxygen O(1)W (open) atoms are shown; all other atoms are omitted for clarity. The hydrogen bonds are shown as thin lines. The crystallographic *c* axis is vertical in the figure.

(37) Cayley, G. R.; Margerum, D. W. *J. Chem. Soc., Chem. Commun.* **1974**, 1002.

of O(3)W within the unit cell. The hydrogen atom on O(3)W was not located. A similar disorder problem with water atoms located at positions along a twofold axis has been reported in the structure of $[Ru(en)_3]Cl_3 \cdot 3.5H_2O$.[38]

Overall, the picture of molecular packing in the crystals of $[Ru(bpy)_2Cl_2] \cdot 3.5H_2O$ is one of neutral ruthenium complexes surrounded by and interacting with pools of water. It should be noted that there is no evidence for "covalent hydrate" formation[39] or for water molecules intercalated between bipyridine rings.

The specific (nonrandom) hydrogen bonding observed may have some structural significance for the state of this and related complexes in hydrogen-bonding solvents. The appearance of specific solvent interactions induced by H bonding could certainly help to explain the breakdown of dielectric continuum theory in attempting to account for solvent effects in optical electron transfer[40] and nonradiative decay.[41]

$[Ru(bpy)_2Cl_2]Cl \cdot 2H_2O$. The crystal structure of this salt is composed of monomeric cationic units balanced by hydrated chloride anions. In contrast to the analogous Ru(II) structure, the coordinated chlorides in the Ru(III) structure are not involved in hydrogen-bonding interactions. The two independent Ru(III)–Cl bond lengths of 2.321 (2) and 2.328 (2) Å (average 2.325 Å) are 0.012–0.022 Å shorter than the Ru(III)–Cl distances trans to NH_3 in the structures of *trans*-(chloro-8-caffeine)chlorotriammineruthenium(III)[42] and $[Ru(NH_3)_5Cl]Cl_2$;[43] they are fully 0.1 Å shorter than the 2.427 (3)-Å Ru(III)–Cl distance trans to the carbene metal bond in the caffeine structure. In contrast, however, the Ru(III)–Cl distances are approximately 0.03 Å longer than the Ru(III)–Cl distance observed in the structure of Ru(benzoato)$(PPh_3)Cl_2$ in which chloride sits trans to the benzoato group.[19] Of particular interest is the marked shortening (~0.1 Å) of the Ru–Cl bond upon oxidation of the metal as observed by comparison of the Ru(II) and Ru(III) structures. A similar decrease in the Ru–Cl bond length upon oxidation at the metal is apparent in the structures of $Ru^{II}Cl(CO)(PPh_3)$(benzoato)[19b] (Ru–Cl = 2.397 (5) Å) and $Ru^{III}Cl_2(PPh_3)$(benzoato)[19a] (Ru–Cl = 2.294 Å) where $\Delta(Ru^{III}-Ru^{II}) = -0.103$ Å.

Effects of ligand electronic asymmetry observed in the Ru(II) structure are, once again, evident in the Ru(III)–N bond distances. The two Ru(III)–N(bpy) bonds trans to Cl, 2.054 (5) and 2.045 (5) Å, are statistically equal and are the shorter of the pair of Ru–N bonds in each ring. In the Ru(II) structure the Ru–N(bpy) bond trans to Cl is also the shorter of the unique pair though the absolute difference between the Ru–N bond distance trans to bpy and the Ru–N distance trans to Cl is decidedly larger within the Ru(II) molecule. This observation again points to the importance of Ru(II)–bpy back-bonding. The Ru(III)–N(bpy) bonds trans to bpy (2.063 (5) and 2.057 (5) Å; average 2.060 (5) Å) are also statistically equal and slightly longer (0.006 Å) than those in the Ru(II) structure but considerably shorter than Ru(III)–N(bpy) bonds reported for other Ru(III) polypyridyl structures. However, the previously reported Ru(III)–polypyridyl structures, e.g. *trans*-$[Ru(bpy)_2(OH)(H_2O)](ClO_4)_2$[44] and $[(NO_2)(bpy)_2Ru-O-Ru(bpy)_2(NO_2)](ClO_4)_2$,[35] suffer from distortions due to ligand arrangement or to Ru–Ru electronic coupling, and there are no appropriate Ru^{III}–pyridyl structures for bond length comparisons.

The very small, perhaps insignificant, difference between the Ru–N(bpy) bond lengths trans to bpy nitrogen in the Ru(II) and Ru(III) structures is reminiscent of the equivalence of Fe–N(phen) bond lengths observed for the tris(phenanthroline)iron(II) and -iron(III) structures[5] and is in marked contrast to changes of 0.09 (2) and 0.04 (1) Å observed upon metal oxidation in the hexaaquaruthenium[7] and hexaammineruthenium[3] couples, respectively. The change in Ru–N(bpy) bond lengths for the nitrogen trans to Cl is, by comparison, drastic with Δ[Ru(III)–Ru(II)] = 0.037 (5) Å. This change is smaller than the difference of 0.07 Å in the Ru–N(pyrazine) bonds of the pentaamine(pyrazine)ruthenium complexes[8] but quite similar to the difference of 0.039 (5) Å in the Ru–N(isonicotinamide) bonds of the tetraaminebis(isonicotinamide)ruthenium(II/III) structures.[2] As in the earlier structures, a striking feature is that, in contrast to the Ru–Cl bond lengths, there is actually a lengthening of the Ru–N bonds in the Ru(III) compared to the Ru(II) complex. This effect would appear to be one more manifestation of the importance of $d\pi-\pi^*$ back-bonding in complexes of Ru(II).

The geometry of the $[Ru(bpy)_2Cl_2]^+$ cation is, like that of its Ru(II) counterpart, very close to octahedral. The bipyridine "bite angles" of 78.5 (2) and 78.8 (2)° are approximately 1° smaller than the analogous angle in the Ru(II) molecule. The cis-chloro angle of 93.7 (1)° is about 4° larger than that in the Ru(II) molecule. The widening of the angle is probably a consequence of increased Cl–Cl repulsion due to the shortening of the Ru–Cl bond in Ru(III) compared to Ru(II). As in the Ru(II) structure, the bipyridine ligands are bent back slightly from coordinated chloride with the trans-N–Ru–N bond angle being 177.3 (2)°. This distortion is, however, 3° less than in the Ru(II) structure.

There are no significant distortions in the bipyridine rings induced by changes in oxidation state at the metal. As in the Ru(II) structure the bipyridine rings in the Ru(III) molecule are planar with maximum deviations from the 12-atom least-squares plane of 0.077 (7) and 0.028 (6) Å for the A and B rings, respectively. The planarity of each individual 6-membered pyridine ring is even more rigorous, with maximum deviations of 0.014 (7) Å (A), 0.018 (5) Å (A′), 0.009 (5) Å (B), and 0.011 (6) Å (B′). The dihedral angles between 6-membered rings within each bipyridine moiety are 5.9° (A–A′) and 1.2° (B–B′), values quite similar to those reported for a variety of bipyridine structures.[35]

Hydrogen bonding within the $[Ru(bpy)_2Cl_2]Cl \cdot 2H_2O$ lattice involves only water and the chloride anion. Metrical parameters are listed in Table V. Channels of hydrated chloride anions run parallel to the *a* axis. Each chloride ion acts as an acceptor of one hydrogen bond from each water. The water oxygen O(1)W in turn acts as an acceptor from O(2)W; however, the second hydrogen attached to O(1)W is apparently not involved in the hydrogen-bonding network. This hydrogen-bonding arrangement has no apparent impact on the structure of the cation.

In contrast to the molecular packing observed in the Ru(II) lattice there are neither stacking interactions nor close contacts in the Ru(III) structure. This result is probably attributable to the ionic nature of the lattice, which necessitates larger separations between ruthenium units.

With the X-ray crystallographic data on $[Ru(bpy)_2Cl_2]$ and $[Ru(bpy)_2Cl_2]^+$ in hand, it is possible to turn to an analysis of the role of intramolecular vibrations on electron-transfer processes involving the couple.

Vibrational Barrier to Electron Transfer. In the classical limit, the vibrational barrier to thermal electron transfer for self-exchange (eq 1) is given by $E_a = \lambda/4$, where λ is the vibrational

$$[(bpy)_2Ru^{II}Cl_2] + [*(bpy)_2Ru^{III}Cl_2]^+ \rightarrow [(bpy)_2Ru^{III}Cl_2]^+ + [*(bpy)_2Ru^{II}Cl_2] \quad (1)$$

reorganization energy.[48] In the harmonic oscillator approximation λ is given by

$$\lambda = \tfrac{1}{2}\sum_j k_j(\Delta Q_j)^2 = \tfrac{1}{2}\sum_j \hbar\omega_j\Delta_j^2 \quad (2)$$

where k_j is the force constant for normal vibration j, ΔQ_j is the difference in equilibrium displacement coordinates between oxidation states for vibration j, $\hbar\omega_j = h\nu_j$ is the quantum spacing between vibrational levels, $\Delta_j = (\Delta Q_j)(M_j\omega_j/\hbar)^{1/2}$ is the dimen-

(38) Peresie, H. J.; Stanko, J. A. *J. Chem. Soc., Chem. Commun.* **1970**, 1674.
(39) Gillard, R. D. *Coord. Chem. Rev.* **1975**, *16*, 67. Walters, W. S.; Gillard, R. D.; Williams, P. A. *Aust. J. Chem.* **1978**, *31*, 1959. Gillard, R. D.; Lancashire, R. J.; Williams, P. A. *J. Chem. Soc., Dalton Trans.* **1979**, 190, 193.
(40) (a) Sullivan, B. P.; Curtis, J. C.; Kober, E. M.; Meyer, T. J. *Nouv. J. Chim.* **1980**, *4*, 643. (b) Curtis, J. C.; Sullivan, B. P.; Meyer, T. J. *Inorg. Chem.* **1982**, *22*, 224.
(41) Caspar, J. V.; Sullivan, B. P.; Kober, E. M.; Meyer, T. J. *Chem. Phys. Lett.* **1982**, *91*, 91.
(42) Krentzen, H. J.; Clarke, M. J.; Taube, H. *Bioinorg. Chem.* **1975**, *4*, 143.
(43) Prout, C. K.; Powell, H. M. *J. Chem. Soc.* **1962**, 137.
(44) Durham, B.; Wilson, S. R.; Hodgson, D. J.; Meyer, T. J. *J. Am. Chem. Soc.* **1980**, *102*, 600.

Table VI. Average Metal–Ligand Bond Lengths in the Complexes *cis*-$[(bpy)_2Ru^{II}Cl_2]$ and *cis*-$[(bpy)_2Ru^{III}Cl_2]^+$

Ru–L	$d(Ru^{II}–L)$, Å	$d(Ru^{II}–L)$, Å	Δd,[a] Å
Ru–Cl	2.426	2.325	0.101
$Ru–N_c$[b]	2.013	2.050	–0.037
$Ru–N_t$[b]	2.054	2.060	–0.006

[a] $\Delta d = d(Ru^{II}–L) - d(Ru^{III}–L)$. [b] For definition of $Ru–N_c$ and $Ru–N_t$, see text.

sionless fractional coordinate difference between oxidation states for vibration j, and M_j is the reduced mass for vibration j. Equation 2 is only approximate since it assumes that the force constant (and angular frequency) of the vibration is the same in both oxidation states.

The total vibrational reorganization energy can be partitioned into an inner-sphere component and an outer-sphere component as in eq 3, where λ_i is the contribution from intramolecular,

$$\lambda = \lambda_i + \lambda_o \tag{3}$$

inner-coordination-sphere vibrations and λ_o is the contribution from collective vibrations of the medium.

The role of solvent in related mixed-valence dimers has been discussed in detail with regard to optical electron transfer.[1,40] Of interest here is the application of the structural information in the previous section to a description of the vibrational barrier to electron transfer. In this regard the salient features revealed by the two structures include the following:

(1) The intraligand bpy bond lengths show no significant differences between the Ru(II) and Ru(III) complexes.

(2) The bpy nitrogens can be divided into two sets of two: those that are trans to another nitrogen (N_t) and those that are trans to a chloride and cis to the other nitrogens (N_c). The average Ru–Cl, $Ru–N_t$, and $Ru–N_c$ bond lengths for the two complexes are given in Table VI.

(3) For the three types of bond length changes—Ru–Cl, $Ru–N_t$, and $Ru–N_c$—the changes in bond distances for each of the two bonds is the same.

(4) For the complex *cis*-$[(bpy)_2Ru^{II}Cl_2]$, there is significant hydrogen bonding between the waters of hydration and the chloride ligands. As mentioned earlier, such specific solvent–ligand interactions may provide a basis for understanding breakdowns in dielectric continuum theory.

The absence of significant changes in the internal structure of coordinated bpy suggests that λ_i is dominated by contributions from modes largely metal–ligand in character. The greatest distortion appears in the Ru^{II}–Cl bond (0.101 Å). The changes in Ru–N bond lengths are $\Delta d(Ru–N_t) = -0.006$ Å and $\Delta d(Ru–N_c) = -0.037$ Å, where $\Delta d(Ru–N) = d(Ru^{II}–N) - d(Ru^{III}–N)$. The difference in $Ru–N_t$ bond lengths is insignificantly small. In terms of contributions to λ_i, it is important to recall that λ_i is proportional to the *square* of the distortion (note eq 2). Therefore, if the trapping normal modes coincided with the stretching of the three sets of motions Ru–Cl, $Ru–N_t$, and $Ru–N_c$, the relative bond length changes of 1 for $Ru–N_t$, 6.2 for $Ru–N_c$, and 16.8 for Ru–Cl would lead to relative contributions to λ_i of 1, 38, and 282, respectively, assuming equal force constants and ligand mass.

The appropriate procedure at this point would be to resolve the observed structural changes between Ru(II) and Ru(III) into contributions from the normal modes largely based on the metal–ligand skeleton. Such an analysis would give ΔQ_{eq} values for the contributing modes and with $\hbar\omega$ values from IR and/or Raman data, the necessary parameters needed for the calculation of λ_i based on eq 3 would be available.

In the absence of a normal-coordinate analysis, we will be forced to make a series of approximations in order to continue the analysis.

A first point to note is that only symmetrical motions of the three sets of donor atoms need be considered given the structural differences between $[Ru^{II}(bpy)_2Cl_2]$ and $[Ru^{III}(bpy)_2Cl_2]^+$. In order to simplify the problem we will treat the bpy ligands as two pyridyl groups and, for the local modes corresponding to stretches of N_t and N_c, we will use a mass of 80 amu.

The model complex *cis*-$[Ru(N_t)_2(N_t)_2Cl_2]$ belongs to the symmetry point group C_{2v} and possesses six metal–ligand stretching modes: $a_1 + b_1$ for $\nu(Ru–N_c)$, $a_1 + b_2$ for $\nu(Ru–N_t)$, and $a_1 + b_1$ for $\nu(Ru–Cl)$. However, only the symmetric a_1 modes need to be considered since for the asymmetric modes (b_1 and b_2), $\Delta Q_{eq} = 0$. As a final assumption, unavoidable in the absence of a normal-coordinate analysis, we will assume that stretches involving the three distinct metal–ligand sets, $\nu_{a_1}(Ru–N_c)$, $\nu_{a_1}(Ru–N_t)$, and $\nu_{a_1}(Ru–Cl)$, represent a reasonable approximation to the actual normal modes. With this assumption the three normal modes can be constructed from the three distinct sets of local modes

$$\Delta Q_e(Ru–N_c) = (1/2^{1/2})[\Delta d(Ru–N_c)_1 + \Delta d(Ru–N_c)_2]$$

$$\Delta Q_e(Ru–N_t) = (1/2^{1/2})[\Delta d(Ru–N_t)_1 + \Delta d(Ru–N_t)_2]$$

$$\Delta Q_e(Ru–Cl) = (1/2^{1/2})[\Delta d(Ru–Cl)_1 + \Delta d(Ru–Cl)_2]$$

or since $\Delta d(Ru–Cl)_1 = \Delta d(Ru–Cl)_2$, etc.

$$\Delta Q_e(Ru–Cl) = (2/2^{1/2})\Delta d(Ru–Cl) = 2^{1/2}\Delta d(Ru–Cl)$$
$$\Delta Q_e(Ru–N_t) = 2^{1/2}\Delta d(Ru–N_t) \tag{4}$$
$$\Delta Q_e(Ru–N_c) = 2^{1/2}\Delta d(Ru–N_c)$$

In the equations above Δd values are the crystallographically derived local bond distance changes. Note that the actual normal modes will consist of linear combinations of the three group-based modes.

The only additional information needed for the application of eq 2 is an estimate of the vibrational frequencies for the metal–ligand modes. Unfortunately vibrational data are somewhat limited, in part, because of the low intensities of the transitions.[45] The symmetric metal–nitrogen stretches for $[Fe^{II}(phen)_3]^{2+}$ and $[Fe^{III}(phen)_3]^{3+}$ have been assigned at 386 and 384 cm^{-1}, respectively,[46] and it is reasonable to expect that the stretching frequencies for the analogous Ru complexes will occur at similar energies. Furthermore, the complexes $[M(bpy)_2Cl_2]$ (M = Pt, Pd, Fe, Co, Zn, Mn) all show symmetric metal–nitrogen stretches in the 357–423-cm^{-1} region.[47] For our calculations, we will assume a symmetric metal–nitrogen stretching frequency of 400 cm^{-1} for both $Ru–N_t$ and $Ru–N_c$.

It is desirable to have a more accurate estimate for the metal–chloride stretching frequencies since λ_i is expected to be dominated by contributions from the M–Cl modes. An infrared spectrum (Nujol) of a microcrystalline sample of *cis*-$[(bpy)_2Ru^{III}Cl_2]Cl$ revealed only two bands in the 200–500-cm^{-1} region at 340 and 422 cm^{-1}, which can be reasonably assigned as the Ru–Cl stretches. We were unable to detect any stretches in this region for *cis*-$[(bpy)_2Ru^{II}Cl_2]$. However, Taube has assigned the Ru–Cl stretches in *cis*-$[(py)_4Ru^{II}Cl_2]$ to bands occurring at 313 and 325 cm^{-1},[49] and we will utilize these values.

As noted above, we require frequencies for the symmetric modes. Although several vibrational analyses of complexes of the type $[L_4MCl_2]^{n+}$ have appeared,[50] we could find no definitive assignments as to which of the metal–chloride stretches is the symmetric stretch. Given the π-donating nature of the Cl^- ligand, the symmetric stretch is expected to be the higher energy mode, since stretching one M–Cl bond should make the second bond stronger on the basis of electrostatic and bonding arguments. In support of the argument, the symmetric M–O stretch in complexes of the type $[L_4MO_2]^{n+}$ complexes is always the higher energy stretch.[51] Finally, since $\hbar\omega_{a_1}(Ru^{II}–Cl) \neq \hbar\omega_{a_1}(Ru^{III}–Cl)$, we

(45) Nakamoto, K. "Infrared Spectra of Inorganic and Coordination Compounds"; Wiley-Interscience: New York, 1970.
(46) Hutchinson, B.; Tokemoto, J.; Nakamoto, K. *J. Am. Chem. Soc.* **1970**, *92*, 3335.
(47) Strukl, J. S.; Walter, J. L. *Spectrochim. Acta, Part A* **1971**, *27A*, 223.
(48) Sutin, N. *Acc. Chem. Res.* **1982**, *15*, 275.
(49) Raichart, D. W.; Taube, H. *Inorg. Chem.* **1972**, *11*, 999.
(50) For example: (a) Clark, R. J. H.; Maresca, L.; Puddephatt, R. J. *Inorg. Chem.* **1968**, *7*, 1603. (b) Clark, R. J. H.; Williams, C. S. *Inorg. Chem.* **1965**, *4*, 350.

Table VII. Vibrational and Structural Data for the Model Complexes *cis*-$[N_4Ru^{II}Cl_2]$ and *cis*-$[N_4Ru^{III}Cl_2]^+$

Ru–L	Δd,[a,b] Å	$\hbar\omega_{a_1}$, cm^{-1}	M_2, amu	Δ(Ru–L), Å
$Ru^{II/III}$–Cl	0.101	364	35.5	2.80
$Ru^{II/III}$–N_c	−0.037	400	80	1.61
$Ru^{II/III}$–N_t	−0.006	400	80	0.26

[a] From Table VI. [b] $\Delta Q_j = N^{1/2}|\Delta d_j|$, where N is the number of Ru–L bonds and Δd is the change in bond distance between oxidation states.

will employ the reduced force constant approach of Sutin.[48] For our treatment, this translates to a reduced symmetric stretch, $\hbar\omega_{a_1}(Ru^{II/III}–Cl)$, given by eq 5.

$$\hbar\omega_{a_1}(Ru^{II/III}–Cl) = \left[\frac{2(\hbar\omega_{a_1}(Ru^{II}–Cl))(\hbar\omega_{a_1}(Ru^{III}–Cl))}{(\hbar\omega_{a_1}(Ru^{II}–Cl))^2 + \hbar\omega_{a_1}(Ru^{III}–Cl))^2}\right]^{1/2} \quad (5)$$

The relevant vibrational and structural data needed to calculate λ_i are summarized in Table VII. From eq 2 and 4, λ_i for thermal electron transfer is given by

$$\lambda_i = \tfrac{1}{2}[2\hbar\omega_{a_1}(Ru^{II/III}–Cl)\,\Delta(Ru^{II/III}–Cl)^2 + 2\hbar\omega_{a_1}(Ru^{II/III}–N_c)\,\Delta(Ru^{II/III}–N_c)^2 + 2\hbar\omega_{a_1}(Ru^{II/III}–N_t)\,\Delta(Ru^{II/III}–N_t)^2] \quad (6)$$

Substituting the values in Table VII into eq 6 yields λ_i = 3920 cm^{-1}. Therefore, in the classical limit, the vibrational barrier to electron transfer from intramolecular modes is given by $\lambda_i/4$ = 980 cm^{-1}.

(51) Jezowska-Trzebiatowska, B.; Hanuza, J. *J. Mol. Struct.* **1973**, *19*, 109.

In fact, the classical limit relies on the assumption that $\hbar\omega << k_BT$. However, for metal–ligand vibrations at room temperature (k_BT = 208.5 cm^{-1} at 25 °C) the classical assumption is clearly inappropriate, and it is important to consider the full quantum treatment. Although our analysis has yielded the necessary parameters to carry out a complete vibrational overlap calculation,[11,12] for self-exchange reactions, the complete result is approximated accurately by eq 7.[10,48] Using the data in Table VII

$$\lambda_{i,QM} = \tfrac{1}{2}\sum_j \hbar\omega_j\Delta_j^2 \frac{4k_BT}{\hbar\omega_j}\tanh\frac{\hbar\omega_j}{4k_BT} \quad (7)$$

gives $\lambda_{i,QM}$ = 3680 cm^{-1}, which is in good agreement with the classical value of λ_i = 3920 cm^{-1}. Our calculations reinforce those made earlier on other metal complexes, which show that at room temperature the classical approximation is adequate to calculate λ_i when vibrational trapping has its origin in low-frequency metal–ligand modes.

Final Comments. The analysis presented here has made an attempt to utilize the results of structural and vibrational analysis to define the intramolecular vibrational barrier to electron transfer for the couple $[Ru(bpy)_2Cl_2]^{+/0}$. Although the results are of interest in their own right, we will return to them later in an attempt to account for the optical electron-transfer properties of related mixed-valence dimers in a detailed way.

Acknowledgment is made to the Army Research Office under Grant No. DAAG29-82-K-0111 for support of this research.

Registry No. *cis*-$[Ru(bpy)_2Cl_2]\cdot 3.5H_2O$, 98014-14-3; *cis*-$[Ru(bpy)_2Cl_2]Cl\cdot 2H_2O$, 98014-15-4.

Supplementary Material Available: Tables of hydrogen atom parameters, thermal parameters, interatomic distances and angles, and values of $10F_o$ and $10F_c$ for *cis*-$[Ru(bpy)_2Cl_2]\cdot 3.5H_2O$ and *cis*-$[Ru(bpy)_2Cl_2]Cl\cdot H_2O$ (38 pages). Ordering information is given on any current masthead page.

Contribution from the Department of Chemistry, University of Virginia, Charlottesville, Virginia 22901

2,2′-Bipyrimidine-Bridged Homobinuclear Complexes

Greg Brewer and Ekk Sinn*

Received November 14, 1984

The synthesis and structural and magnetic properties of a series of 2,2′-bipyrimidine- (Bpm-) bridged binuclear complexes $L_2M(Bpm)ML_2$ of Mn(II), Co(II), and Ni(II) are reported, where L = $F_3CC(O)CHC(O)CF_3$ (hfa), $F_3CC(O)CHC(O)CH_3$ (tfa), and $F_3CC(O)CHC(O)C_6H_5$ (Phtfa). Mass spectroscopic observation of the $[ML_2(Bpm)]^+$ or $[ML_2(Bpm) - F]^+$ ions distinguishes the binuclear complexes from the mononuclear adducts. The complexes all exhibit antiferromagnetic exchange with a maximum in the magnetic susceptibility in the 18–23 K region for the Ni(II) complexes and in the 13–16 K region for the Co(II) complexes with L = tfa and Phtfa. The structure of one of the complexes, $(hfa)_2Co(Bpm)Co(hfa)_2$, is reported. It is monoclinic, $P2_1/n$, with Z = 2, a = 8.790 (3) Å, b = 17.980 (4) Å, c = 12.490 (6) Å, and β = 102.76 (3)°. The structure was refined to a R value of 4.9%. The two equivalent cobalt atoms are each bound to four hfa oxygens and two cis nitrogens of the Bpm in a slightly distorted octahedral environment. The cobalt atoms are 0.09 Å out of the Bpm plane, which provides favorable overlap of the metal $d_{x^2-y^2}$ orbitals with the ligand π system, allowing magnetic exchange to occur. The metal–metal separation is 5.750 (2) Å, the cobalt–oxygen bonds average 2.051 Å, and the cobalt–nitrogen bonds are 2.150 (3) Å.

Introduction

There has been great interest in the area of binuclear transition-metal complexes in recent years.[1-5] In part this stems from the fact that binuclear complexes have been found to occur in a number of metalloenzymes.[6] The influence of structure on magnetism of synthetic binuclear complexes is useful in assessing structurally unknown systems. Also of interest are the structural and electronic factors that contribute to the magnetic exchange interactions.

Homobinuclear complexes are more common than heterobinuclear ones and have been studied to a greater extent. Homobinuclear complexes can be symmetric, having identical donor atoms for each metal, or asymmetric arising from nonequivalent donor sets (e.g. **1**) or by accidental addition of a monodentate ligand to one of two equivalent donor sets[7] (**2**). Symmetric complexes occur in some salts such as copper acetate,[8] $[Cu(R\text{-}sal)Cl]_2$ (**3**), and $[Ni(R\text{-}sal)NO_3L]_2$[10] (**4**) (L = solvent), or they

(1) (a) Gruber, S. J.; Harris, C. M.; Sinn, E. *Inorg. Chem.* **1968**, *7*, 268. (b) *Ibid. J. Inorg. Nucl. Chem.* **1968**, *30*, 1805.
(2) Castello, U.; Vigato, P. A.; Viladi, M. *Coord. Chem. Rev.* **1977**, *23*, 31.
(3) Sinn, E.; Harris, C. M. *Coord. Chem. Rev.* **1969**, *4*, 391.
(4) Hodgson, D. P. *Prog. Inorg. Chem.* **1974**, *19*, 173.
(5) Krautil, P.; Robson, R. J. *Coord. Chem.* **1980**, *10*, 7.
(6) Kurtz, D. M., Jr.; Shriver, D.; Klotz, I. M. *Coord. Chem. Rev.* **1977**, *24*, 145.
(7) Butcher, R. J.; Devan, G.; Mockler, G. M.; Sinn, E., submitted for publication.
(8) Van Niekerk, J. H.; Schoenig, F. R. L. *Acta Crystallogr.* **1953**, *6*, 227. De Meester, P.; Fletcher, S. R.; Skapski, A. C. *J. Chem. Soc., Dalton Trans.* **1973**, 2575.

0020-1669/85/1324-4580$01.50/0